A high-resolution study of Holocene paleoclimatic and paleoceanographic changes in the Nordic Seas

Bjørg Risebrobakken,[1] Eystein Jansen,[1,2,3] Carin Andersson,[2]
Eirik Mjelde,[1] and Kjersti Hevrøy[1,4]

Received 31 January 2002; revised 29 October 2002; accepted 5 November 2002; published 26 March 2003.

[1] High-resolution records from IMAGES core MD95-2011 in the eastern Norwegian Sea provide evidence for relatively large- and small-scale high-latitude climate variability throughout the Holocene. During the early and mid-Holocene a situation possibly driven by consistent stronger westerlies increased the eastward influence of Arctic intermediate and near-surface waters. For the late Holocene a relaxation of the atmospheric forcing resulted in increased influence of Atlantic water. The main changes in Holocene climate show no obvious connection to changing solar irradiance, and spectral analysis reveals no consistent signature for any periodic behavior of Holocene climate at millennial or centennial timescales. There are, however, indications of consistent multidecadal variability. *INDEX TERMS:* 4267 Oceanography: General: Paleoceanography; 3344 Meteorology and Atmospheric Dynamics: Paleoclimatology; 4870 Oceanography: Biological and Chemical: Stable isotopes; *KEYWORDS:* Holocene, climate, Nordic Seas, NAO, high resolution, variability

Citation: Risebrobakken, B., E. Jansen, C. Andersson, E. Mjelde, and K. Hevrøy, A high-resolution study of Holocene paleoclimatic and paleoceanographic changes in the Nordic Seas, *Paleoceanography*, *18*(1), 1017, doi:10.1029/2002PA000764, 2003.

1. Introduction

[2] The Holocene has been considered a period characterized by relatively stable climate conditions, a view largely based on the stability of the Holocene $\delta^{18}O$ from the Greenland ice core compared to the glacial parts [*Grootes et al.*, 1993]. An emerging picture of more variable high northern latitude climates is indicated by a number of recent studies [e.g., *Dahl and Nesje*, 1996; *Bond et al.*, 1997; *Bianchi and McCave*, 1999; *Bond et al.*, 2001]. However, the nature of this variability and the possible driving mechanisms are still to a large extent unresolved. It has been debated whether the Holocene climatic and oceanographic changes have the same general characteristics as the millennial scale climate fluctuations of the last glacial period, only with a subdued amplitude, or if other characteristics and driving forces were responsible for the evolution of climate during the current interglacial period. Several papers claim that there is a substantial ~1500 year periodicity throughout the Holocene, being the source of cold spells documented in different proxy records [*Bond et al.*, 1997; *Mayewski et al.*, 1997; *Campbell et al.*, 1998; *Bianchi and McCave*, 1999]. Other studies question this result, and evidence in favor of a more prominent 900–1000 and 550 year Holocene periodicity also exists, both from ice core and marine records [*Stuvier and Braziunas*, 1993; *Stuvier et al.*, 1995; *Grootes and Stuiver*, 1997; *Schulz and Paul*, 2002; *Chapman and Shackleton*, 2000]. *Bond et al.* [2001] argue that Holocene climate variability is connected to changing solar irradiance, and that the centennial scale variability seen (on the order of 200–500 years) does not reflect any strict periodic climate behavior. Rather, clusters of these changes are argued to produce the previously reported 1500-year variability [*Bond et al.*, 1997].

[3] For the North Atlantic there is evidence of a possible connection between longer term Holocene climate changes and periods of a relatively consistent state of the atmospheric pressure system over the North Atlantic region [*Barlow et al.*, 1997; *Keigwin and Pickart*, 1999; *Schulz and Paul*, 2002; *Nesje et al.*, 2000; *deMenocal et al.*, 2000]. Here we provide evidence bearing on these issues from high-resolution foraminiferal $\delta^{18}O$ and foraminiferal census records from the Vøring Plateau in the eastern Norwegian Sea (Figure 1).

2. Material and Methods

[4] The material in this study was obtained from IMAGES piston core MD95-2011 and box core JM97-948/2A (66°58.19N, 07°38.36E and 1048 m water depth) (Figure 1). The cores were spliced to develop a continuous record throughout the Holocene, as MD95-2011 did not recover the youngest part. The last 564 cal. years BP are represented by JM97-948/2A. Box core JM97-948/2A was sampled every half cm from 0–30 cm and MD95-2011 is sampled every cm from 0–745 cm.

2.1. Chronology

[5] The chronology is based on linear interpolation between dated levels. The age control for box core JM97-948/2A is based on nine ^{210}Pb and two Accelerator Mass

[1]Department of Earth Science, University of Bergen, Bergen, Norway.
[2]Bjerknes Centre for Climate Research, University of Bergen, Bergen, Norway.
[3]Also at Nansen Environmental and Remote Sensing Centre (NERSC), Bergen, Norway.
[4]Now at Norsk Hydro ASA, Bergen, Norway.

0883-8305/03/2002PA000764$12.00

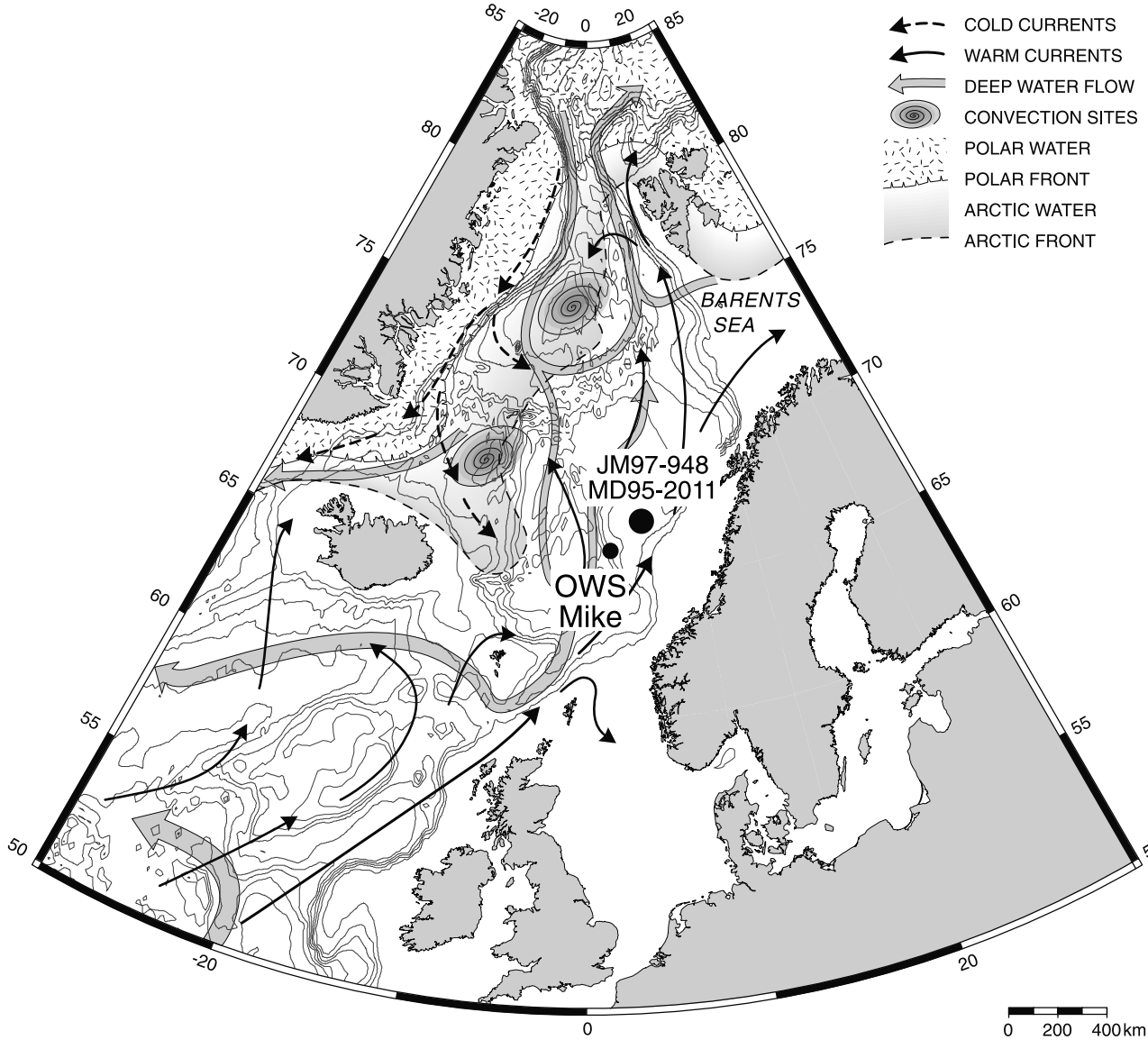

Figure 1. Map showing the location of cores JM97-948/2A and MD95-2011. The main current systems of the region are also shown.

Spectrometry (AMS) ^{14}C dates. To provide a better fit between the ^{14}C AMS ages of the two cores, ^{210}Pb ages below 10.5 cm in the box core were not used. The decay time of 210Pb ($t_{1/2}$ = 22.26 years) [*Appleby and Oldfield*, 1992] also implies that those dates are less certain. The established age model for MD95-2011 rests on twelve ^{14}C AMS dates and the presence of the Vedde ash layer. Two additional AMS ^{14}C dates were not used as they gave inverted ages probably related to resedimentation. One other date, inverted (overlapping age range) compared to the Vedde ash, was also omitted as the Vedde ash age is presumed to be more reliable. The radiocarbon ages were all measured on *Neogloboquadrina pachyderma*. The AMS ^{14}C ages are corrected for a marine reservoir effect of 400 years and converted to calendar ages by using Calib 4.3 [*Stuvier et al.*, 1998]. All ages are given in calendar years BP 2000 (Figure 2; Table 1). For the late Holocene part of the sequence, we consider the age control to be good. In the earlier parts of the record the accuracy of the age scale is less certain, as fewer dates exist due to a low foraminifera content in the sediment. The possible age ranges of the oldest dates also increase due to the ^{14}C plateaus that characterize this interval (Table 1) [*Stuiver et al.*, 1998]. The average sedimentation rate of the spliced sequence is about 56 cm/kyr.

2.2. Stable Oxygen Isotopes

[6] Oxygen isotope measurements were performed at the GMS lab at the University of Bergen, using Finnigan MAT 251 and MAT 252 mass spectrometers both equipped with automatic preparation lines (“Kiel device”). Records were obtained for both left and right coiling forms of the planktic foraminifer *N. pachyderma* and from the benthic foraminifer *Cassidulina teretis* (normally 12–17 specimens of *N.*

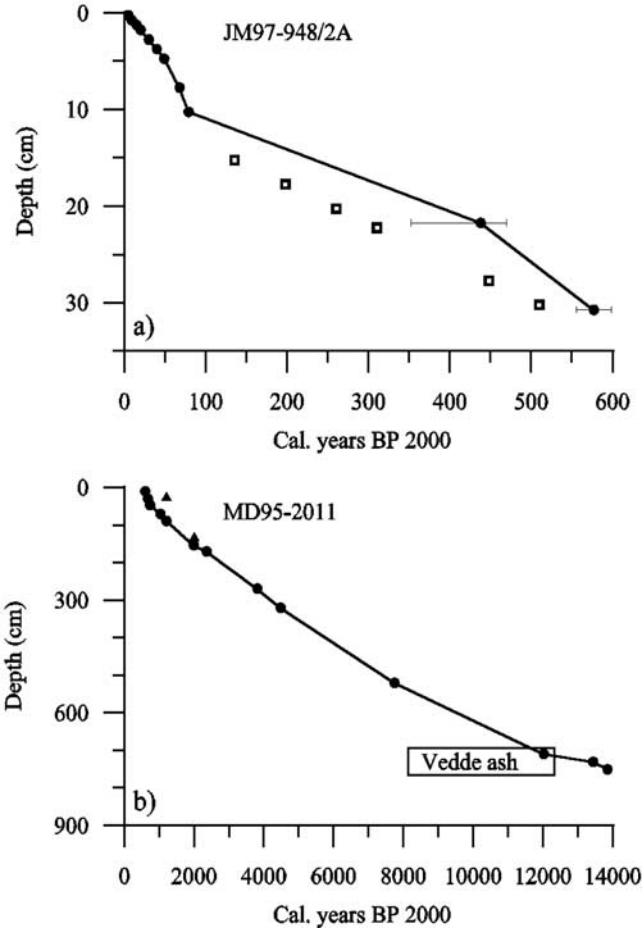

Figure 2. (a) Age model for JM97-948/2A. Circles represent ^{210}Pb and ^{14}C dates used in the age model, squares represent ^{210}Pb dates not used in the age model. (b) Age model for MD95-2011. ^{14}C dates used in the age model and the Vedde ash layer are indicated by circles. Triangles represent ^{14}C dates not used.

pachyderma and 15–20 specimens of *C. teretis*; 150–500 μm). Samples were crushed and cleaned with methanol in an ultrasonic bath before being measured. The reproducibility of the analyses is ±0.07‰ for the oxygen isotope measurements, based on replicate measurements of carbonate standards. All results are reported as δ^{18}O in ‰ vs. PDB, using NBS 19. A 5-pt running average was run to smooth the δ^{18}O records. In the text, all reference is to the smoothed δ^{18}O if not otherwise noted. We corrected the δ^{18}O records for the ice volume effect, based on the results of *Fairbanks* [1989], where 10 m sea level equals 0.11‰ δ^{18}O (Figure 3). Sampling every cm makes the mean temporal resolution 15–27 years.

2.3. Foraminiferal Abundance and SST Estimation

[7] The relative abundance of planktic foraminifers is based on census counts of splits of the >150 μm fraction containing approximately 300 planktic foraminifers. Samples were counted at 5 cm intervals for this portion of the study. The planktic foraminifer fauna is characterized by polar, subpolar and transitional species. The dominant species are *N. pachyderma* (dex) and *Globigerina quinqueloba*. Other species, including *N. pachyderma* (sin), *Globigerina bulloides*, *Globigerinita glutinata* and *Globorotalia inflata*, are found in lower abundance in virtually all samples.

[8] Here we present sea surface temperature (SST) estimates for the past 13.6 kyr based on the modern analogue technique (MAT) in conjunction with the ATL916 core-top database (U. Pflaumann, personal communication, 2000). SSTs were calculated based on interpolated modern SSTs at 10-m water depth for August according to *Levitus* [1994]. The MAT SST estimates are based on the 10 best analogues, using the squared chord distance as the dissimilarity measure. Counting every 5 cm gives a mean temporal resolution of 75–135 years.

2.4. Time Series Analysis

[9] The existence of possible periodic or quasiperiodic behavior of the Holocene climate has been investigated by performing time series analyses on the three oxygen isotope records and on the record of relative abundance of *N. pachyderma* (sin.). Time series results were obtained by the Blackman-Tukey Method [*Blackman and Tukey*, 1958] of spectral estimation using the *AnalySeries* software [*Paillard et al.*, 1996]. The records were initially prepared by removing linear trends and resampling at constant 20-year intervals for the stable isotope records and 100-year intervals for the percentage of *N. pachyderma* (sin.). The confidence interval was set at 90%. Similar results (not shown) were also obtained using the MultiTaper Method [*Thompson*, 1982] and the Maximum Entropy Method [*Haykin*, 1983]. To recognize possible nonstationarity through time, the interval from 11.5 ka BP to the present was investigated first; thereafter 6 ka slices of the records (11.5-6 ka BP, 10-4 ka BP, 8-2 ka BP and 6 ka BP to recent) were run with the same settings.

3. Results

3.1. Planktic δ^{18}O

[10] While an overall comparison of the planktic isotope records shows some individual differences the major trends are clearly related. The records indicate three different intervals of distinct Holocene variability: the time interval ranging from glacial termination to about 8 ka BP, from ~8 ka BP to ~3–4 ka BP, and from ~3–4 ka BP to the present (Figure 3).

[11] At about 11.6 ka BP, the planktic δ^{18}O values stabilized at an interglacial level after a rather rapid transition from the Younger Drays (Figure 3b). After about 10.6 ka BP, there is a gradual trend toward increased δ^{18}O, terminating just before 8 ka BP in the highest values of the entire Holocene. This event is most pronounced in the *N. pachyderma* (sin.) record (0.70‰ enrichment (raw data)), but has a broader and less distinct expression in the dextral record (Figure 3b). Throughout the early Holocene, the contrast between dextral and sinistral δ^{18}O (planktic $\Delta\delta^{18}$O) was reduced relative to the younger parts of the Holocene (Figure 4a; Table 2). The mid-Holocene was a more stable period, characterized by small-scale

Table 1. Summary of Tie Points Used to Establish the Age Models for JM97-948/2A and MD95-2011[a]

Identifier	Core	Depth, cm	Material Dated	Submitted Sample Size	Age ^{14}C AMS ± 1σ	Cal. Age BP(2000)	Age Range ±1σ	Comments
	JM97-948/2A	0.25				5		^{210}Pb dated
	JM97-948/2A	0.75				9		^{210}Pb dated
	JM97-948/2A	1.25				15		^{210}Pb dated
	JM97-948/2A	1.75				20		^{210}Pb dated
	JM97-948/2A	2.75				30		^{210}Pb dated
	JM97-948/2A	3.75				40		^{210}Pb dated
	JM97-948/2A	4.75				49		^{210}Pb dated
	JM97-948/2A	7.75				68		^{210}Pb dated
	JM97-948/2A	10.25				79		^{210}Pb dated
KIA 6285	JM97-948/2A	21.75	NPD[b]	8.24 mg	735 ± 40	448	362–480	
KIA 4800	JM97-948/2A	30.75	NPD	8.01 mg	940 ± 40	579	558–601	
GifA96471	MD95-2011	10.5	NPD	8.94 mg	980 ± 60	601	568–675	
KIA 5600	*MD95-2011*	*24.5*	*NPD*	*8.5 mg*	*1590 ± 40*	*1209*	*1150–1237*	not used
KIA 3925	MD95-2011	30.5	NPD	8.6 mg	1040 ± 40	675	614–695	
KIA 5601	MD95-2011	47.5	NPD	8.4 mg	1160 ± 30	739	716–772	
KIA 3926	MD95–2011	70.5	NPD	8.2 mg	1460 ± 50	1037	993–1103	
KIA 6286	MD95-2011	89.5	NPD	8.76 mg	1590 ± 30	1209	1169–1227	
KIA 3927	*MD95-2011*	*130.5*	*NPD*	*7.2 mg*	*2350 ± 40*	*2012*	*1965–2052*	not used
KIA6287	MD95-2011	154	NPD	10.55 mg	2335 ± 25	1992	1965–2047	
GifA96472	MD95-2011	170.5	NPD	7 mg	2620 ± 60	2359	2322–2392	
KIA 10011	MD95-2011	269.5	NPD	7.7 mg	3820 ± 35	3813	3748–3870	
KIA 463	MD95-2011	320.5	NPD	11 mg	4330 ± 50	4484	4449–4563	
KIA 464	MD95-2011	520.5	NPD	6.9 mg	7260 ± 60	7747	7706–7817	
TUa-3315	*MD95-2011*	*703.5*	*NPS*[b]	*7.0 mg*	*10775 ± 85*	*12142, 12067, 12018*	*11761–12394*	not used (Vedde age supposed to be less uncertain)
	MD95-2011	709.5				12030		Vedde ash
TUa-3316	MD95-2011	730.5	NPS	5.1 mg	11875 ± 140	13443	13114–13825	
KIA 465	MD95-2011	750.5	NPS	10 mg	12220 ± 90	13856	13496–13889	

[a]The ^{14}C AMS dates were measured at the Leibniz-Labor for Radiometric Dating and Isotope Research, Kiel (KIA), Centre des Faibles Radioactivités, Gif sur Yvette (GifA) and at Laboratoriet for Radiologisk Datering, Trondheim (TUa). The age of the Vedde ash layer is the GRIP age from *Grönvold et al.* [1995].
[b]NPD: *N. pachyderma* (dex.); NPS: *N. pachyderma* (sin).

variability superimposed on a slightly increasing δ^{18}O trend (*N. pachyderma* (dex.) δ^{18}O: 1.1‰ to 1.7‰ (7800-3900 ka BP); *N. pachyderma* (sin.) δ^{18}O: 1.8‰ to 2.2‰ (7600-3800 ka BP)) (Figure 3b). The planktic $\Delta\delta^{18}$O was somewhat larger than during the early Holocene (Figure 4a; Table 2). More pronounced variability characterizes the late Holocene (Table 2). Here the generally decreased δ^{18}O was interrupted by shorter events of increased δ^{18}O (Figure 3b). The planktic $\Delta\delta^{18}$O is somewhat higher than during the mid-Holocene, interrupted by shorter periods of reduced values (Figure 4a).

3.2. Benthic δ^{18}O

[12] Shifts in the benthic record of δ^{18}O of up to 0.8‰ occur, and 0.3‰ variability is seen frequently, indicating nonstable deep water conditions at the Vøring Plateau during the Holocene. Intervals of decreased benthic δ^{18}O appear to correspond to periods of increased planktic δ^{18}O, and vice versa (Figure 3b). Both planktic-benthic $\Delta\delta^{18}$O records clearly reflect this relationship (Figure 4b). At about 3.6-2.8 ka BP there is a transition zone after which the planktic and benthic records seem to be in phase, in contrast to the earlier portion of the Holocene.

[13] In the period before 9.8 ka BP, benthic δ^{18}O decreased by more than 0.1‰ compared to modern values (4.1‰). During the Younger Drays, an even more extreme interval of decreased δ^{18}O occurred (Table 2). From 9.8-3.5 ka BP, there was a gradual evolution from slightly increased (4.3‰) to much more decreased (3.6‰) δ^{18}O than today. Increased δ^{18}O values characterize the last 2.8 kyr BP, interrupted by shorter periods of decreased δ^{18}O (Figure 3b).

3.3. Foraminifera and SST Records

[14] Prior to 11.7 ka BP, the *N. pachyderma* (sin.) content was high and stable at about 95% (Figure 5a). Subsequently, the relative abundance of *N. pachyderma* (sin.) decreased with the termination of glacial conditions, and after about 10.5 ka BP it stabilized at interglacial values. The average relative abundance between 10.5-3.5 ka BP is 23%, with an increasing percentage marking the cold event at ~8 ka BP. For the late Holocene, even lower percentages are recorded (Table 2). There is a high degree of correlation between the estimated MAT SST and the relative abundance of *N. pachyderma* (sin.), the correlation coefficient being 0.89. A slight warming trend observed in the MAT SST during the mid-Holocene might be seen as a contradiction to the other temperature indicators (Figure 5b). This appears to be due to an increase in the abundance of the dextral coiling form of *N. pachyderma*, a trend not recorded by *N. pachyderma* (sin.) and *G. quinqueloba* (Figures 5b–5e). These three species together comprise >88% of the total amount of planktic foraminifers. Low abundances of *G. quinqueloba* characterize the period prior to 10.5 ka BP. From then on this taxon increases in abundance and

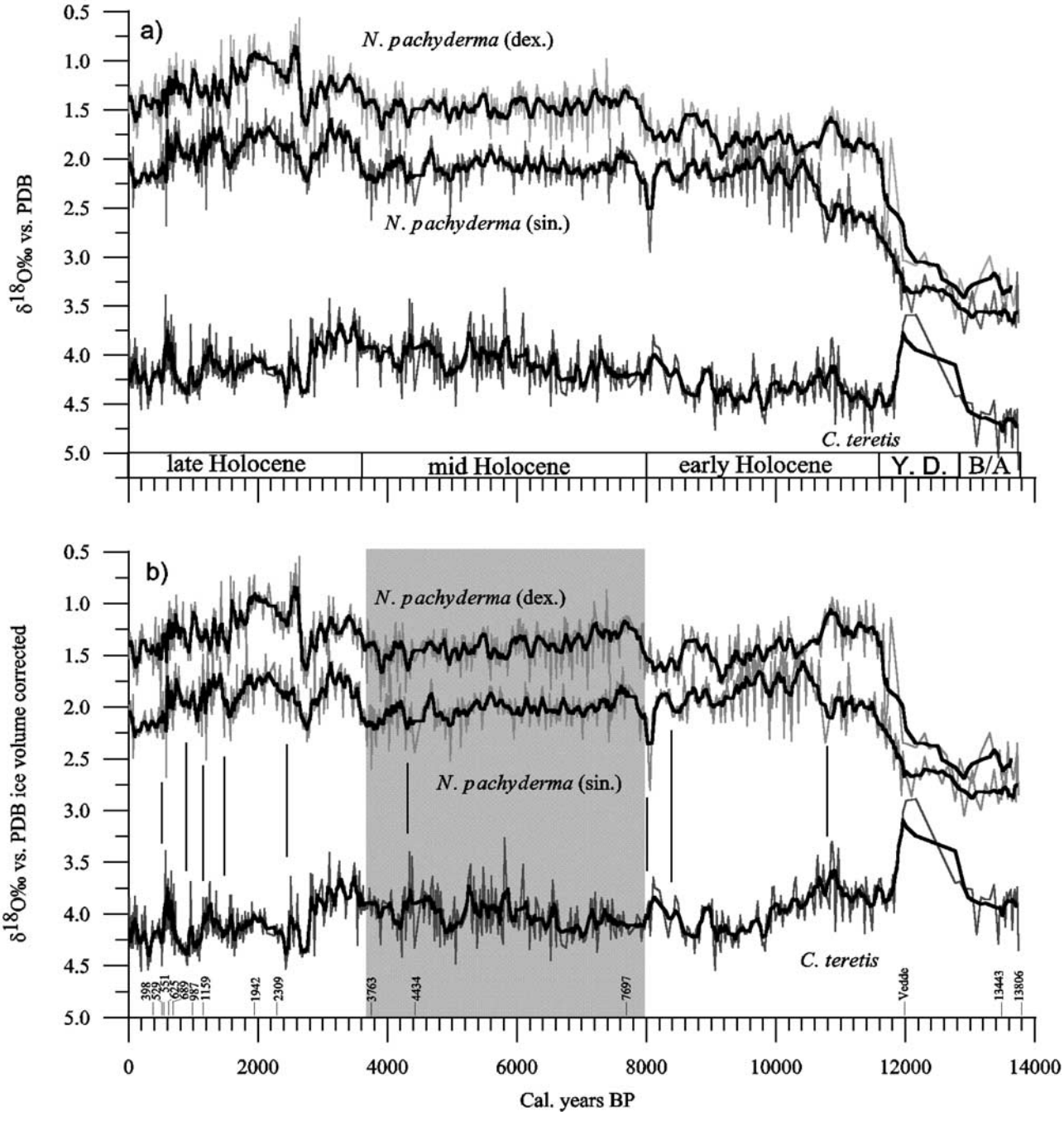

Figure 3. (a) Oxygen isotope records in ‰ vs. PDB. Thick black lines show the 5 point running average of the records. (b) Ice volume corrected $\delta^{18}O$. Tie points for the age model are indicated at the bottom of the graph. Green lines indicate events of inversion between the planktic and the benthic signals. Y.D.: Younger Drays. B/A: Bølling-Allerød.

maximum values characterize the mid-Holocene. During the late Holocene, the abundances are lower. High-amplitude events are seen frequently on shorter timescales throughout the last ~9 kyr (Figure 5d; Table 2).

3.4. Time Series Analysis

[15] Time series analysis reveals evidence for weak periodicities on decadal, centennial and millennial timescales. It should be noted that the particular periodicities reported are spectral peaks (local maxima in the power spectra) that may represent broad bands of quasiperiodic variability rather than narrow, well defined periodicities. The *N. pachyderma* (sin.) $\delta^{18}O$ record shows concentrations of variance at 1150- and 550-year periodicities. The 1150-year period is most pronounced in the intervals 8-2 ka BP and 6-0 ka BP, while the 550-year period is better expressed in the intervals 11.5-

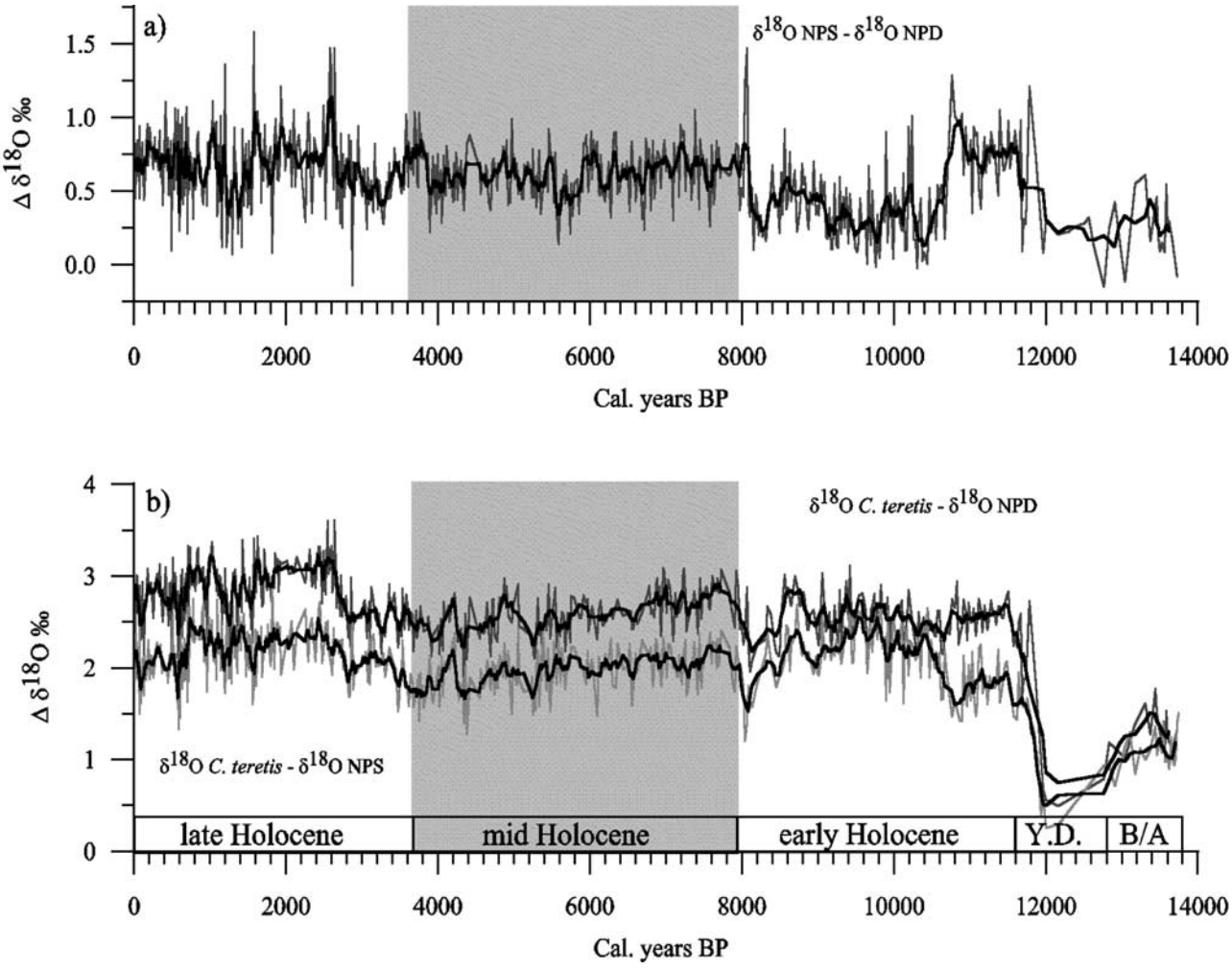

Figure 4. (a) Changes in the contrast between δ^{18}O of *N. pachyderma* (dex.) and *N. pachyderma* (sin.). (b) Changes in the contrasts between planktic δ^{18}O and benthic δ^{18}O. Y.D.: Younger Drays. B/A: Bølling-Allerød.

6 ka BP and 10-4 ka BP. A strong 115-year signal is also seen in the interval 11.5-6 ka BP (Figure 6a). In the record of *N. pachyderma* (dex.) δ^{18}O, evidence of a 1250-year period is seen. The signal is stronger in the 6-0 ka BP interval than in the 11.5-6, 10-4 and 8-2 ka BP intervals. From 8-2 ka BP, a 417-year period is also seen, while the interval between 11.5-6 ka BP records a relatively strong 115-year signal (Figure 6b). Time series results from % *N. pachyderma* (sin.) indicate a 1400-year periodic imprint, and for the 11.5-6 ka BP interval a 570-year signal (Figure 6d). The *C. teretis* δ^{18}O record shows a periodicity of 900 years, but only for the 11.5-6 and the 10-4 ka BP intervals. A significant 260-year signal is also seen in the benthic δ^{18}O. It is very well represented between 10-4 ka BP and also well recorded in the 11.5-6 and the 8-2 ka BP interval. In the 11.5-6 ka BP interval, a 115-year signal exists (Figure 6c). Lower frequency signals can not be reliably distinguished as the length of their periods are too long compared with the length of the investigated intervals. Each δ^{18}O record indicates periodic behavior around 81 years, which appears to be consistent through time, except for the 8-2 ka BP interval in the *N. pachyderma* (dex.) δ^{18}O, where only a very weak signal is seen.

4. Discussion

4.1. Holocene Paleoclimatic and Paleoceanographic Evolution

[16] Correcting the individual δ^{18}O records for the ice volume effect relates the remaining signal to changes in temperature and salinity. Different salinity-δ^{18}O relationships were considered in order to estimate the relative influence of salinity versus temperature. Traditionally, the North Atlantic mixing line [*Craig and Gordon*, 1965] has been used as a standard for the Nordic Seas, giving a steep salinity/δ^{18}O gradient due to the negative freshwater end-member (−21‰). As the local hydrological regime of the Nordic Seas may include several sources of freshwater (precipitation, Arctic river influx, melting sea ice) with less negative isotopic compositions, the freshwater end-member will probably not be the same as for the North Atlantic mixing line. Today's situation gives a gradient of 0.6‰ $\delta^{18}O_w$ per

Table 2. Mean, Maximum, and Minimum Values (Raw Data) are Presented for Each Time Interval of the Records

	Late Holocene, 0–3.6 ka BP			Mid-Holocene, 3.6–7.9 ka BP		
	Mean ±1σ	Maximum Value	Minimum Value	Mean ±1σ	Maximum Value	Minimum Value
$\delta^{18}O$ *N. pachyderma* (dex)	1.27 ± 0.22	2.15	0.54	1.4 ± 0.17	1.94	0.87
$\delta^{18}O$ *N. pachyderma* (sin)	1.94 ± 0.21	2.68	1.28	2.02 ± 0.15	2.6	1.61
$\delta^{18}O$ *C. tereis*	4.09 ± 0.23	4.55	3.39	4.00 ± 0.21	4.48	3.27
$\Delta\delta^{18}O$ (*N. pach.* (sin)-*N. pach.* (dex))	0.66 ± 0.24	1.58	0.14	0.62 ± 0.17	1.05	0.14
$\Delta\delta^{18}O$ (C. teretis-*N. pach.* (dex))	2.81 ± 0.29	3.61	2.11	2.58 ± 0.23	3.09	1.76
$\Delta\delta^{18}O$ (C. teretis -*N. pach.* (sin))	2.15 ± 0.27	2.91	2.34	1.97 ± 0.23	2.43	2.19
% *N. pachyderma* (sin)	14.20 ± 6.75	30.53	3.8	21.83 ± 8.18	44	8.68
N. pachyderma (dex)/g	80.23 ± 71.93	387.97	3.98	72.17 ± 56.10	308.06	4.89
N. pachyderma (sin)/g	17.49 ± 14.37	70.46	1.31	40.41 ± 27.97	180.29	6.51
G. quinqueloba./g	28.52 ± 24.20	118.55	1.72	52.85 ± 24.27	107.46	6.97
MAT SST	11.06 ± 0.76	11.93	8.88	10.20 ± 0.78	11.51	8.5
	Early Holocene, 7.9–11.6 ka BP			Bølling-Allerød/Younger Drays, 11.6–13.8 ka BP		
	Mean ±1σ	Maximum Value	Minimum Value	Mean ±1σ	Maximum Value	Minimum Value
$\delta^{18}O$ *N. pachyderma* (dex)	1.42 ± 0.20	1.8	0.95	2.31 ± 0.44	2.9	1.14
$\delta^{18}O$ *N. pachyderma* (sin)	1.90 ± 0.23	2.1	1.4	2.64 ± 0.26	3.05	1.96
$\delta^{18}O$ *C. tereis*	3.96 ± 0.23	4.54	3.3	3.76 ± 0.31	4.34	2.89
$\Delta\delta^{18}O$ (*N. pach.* (sin)-*N. pach.* (dex))	0.47 ± 0.29	1.47	0.03	0.39 ± 0.50	2.74	0.15
$\Delta\delta^{18}O$ (C. teretis-*N. pach.* (dex))	2.55 ± 0.23	3.12	1.94	1.44 ± 0.57	2.73	0.5
$\Delta\delta^{18}O$ (C. teretis-*N. pach.* (sin))	2.08 ± 0.33	3.29	2.09	1.14 ± 0.37	2.38	1.04
% *N. pachyderma* (sin)	29.38 ± 15.26	80.78	10.84	94.82 ± 14.29	96.88	92.67
N. pachyderma (dex)/g	36.50 ± 54.50	347.11	7.64	3.24 ± 1.56	6.52	0.87
N. pachyderma (sin)/g	39.14 ± 85.73	536.16	4.13	104.07 ± 29.94	138.52	45.06
G. quinqueloba./g	20.66 ± 14.66	62.24	2.12	1.64 ± 0.78	3.58	0.58
MAT SST	10.22 ± 0.87	11.57	6.27	3.93 ± 1.04	4.69	2.96

practical salinity unit (PSU) for the North Atlantic mixing line, compared with 0.2–0.3‰ $\delta^{18}O_w$ per PSU for the Nordic Seas mixing line [*Østbø*, 2000]. Observations from the Svinøy section (NW from 62°N on the Norwegian coast to 64°40N) show that the maximum salinity of the inflowing Atlantic water is about 35.25‰ (100 m depth) [*Mork and Blindheim*, 2000]. The Arctic intermediate water has a defined salinity between 34.87‰ and 34.91‰ [*Blindheim*, 1990]. Given these two sources, a possible change in salinity at the studied site is estimated to be in the range of about 0.38‰ PSU for the Holocene, corresponding to 0.08–0.23‰ change in $\delta^{18}O_w$ depending on the preferred mixing line. The study site location should be more closely related to the Nordic Seas mixing line, so the lower values are more likely. Thus the main features of the planktic isotope records are more likely related to variations in temperature than salinity.

[17] In Arctic water there is no difference between $\delta^{18}O$ values obtained from *N. pachyderma* (sin.) and *N. pachyderma* (dex.), while the differences increase going eastward in the Nordic Seas and into warmer Atlantic water masses [*Johannessen*, 1992]. Thus the varying contrast between the $\delta^{18}O$ of *N. pachyderma* (dex.) and *N. pachyderma* (sin.) can be used as an indicator of horizontal migration of the Arctic water/Atlantic water interface (Arctic Front). *Globigerina quinqueloba* is a species whose distribution is closely related to the Arctic front area [*Johannessen et al.*, 1994]. The low planktic $\Delta\delta^{18}O$ and the high *G. quinqueloba* content indicate that site MD95-2011 was closer to the Arctic front and Arctic water masses during the early and mid-Holocene than during the late Holocene (Figures 4 and 5).

[18] A similar situation has emerged during recent decades because sustained strong westerlies have led to an eastward migration of the subsurface Arctic water [*Blindheim et al.*, 2000]. Based on the combined isotopic and *G. quinqueloba* evidence, we suggest that the apparently stronger influence of Arctic water in the early and mid-Holocene was the result of more pervasive strong westerlies. *Harrison et al.* [1992] used an atmospheric general circulation model to simulate the climatic influence of insolation changes throughout the Holocene and found that, during the early and mid-Holocene, the Icelandic Low and the westerly jet stream were displaced further north, producing mild and wet winters in northern Europe. A reconstruction of mean winter precipitation in the Jostedalsbreen area of western Norway indicates higher winter precipitation during early and mid-Holocene [*Nesje et al.*, 2000]. The same period is characterized by cold reconstructed SST and a high trade wind activity at ODP Site 685C off Cap Blanc, west Africa [*deMenocal et al.*, 2000]. An antiphase relationship between temperature anomalies between Greenland and Scandinavia has also been observed during parts of this period [*Schulz and Paul*, 2002]. All situations might be similar to a positive North Atlantic Oscillation (NAO)-like situation [*Hurrell*, 1995].

[19] A striking feature of the foraminiferal based records from site MD95-2011 is the lack of evidence for the early Holocene warm optimum, well known from marine and terrestrial records [*Karlén*, 1988; *Koç Karpuz and Jansen*, 1992; *Koç et al.*, 1993; *Nesje and Dahl*, 1993; *Lubinski et al.*, 1999]. However, SST estimates from the same site based on diatom abundance and U_{37}^{K} analysis do record the warmth optimum [*Birks*, 2001; *Calvo et al.*, 2002]. This discrepancy between phytoplankton and foraminiferal based proxies may be due to the fact that eastward migration of Arctic water, forced by stronger westerlies, tends to preferentially influence the subsurface water, not the uppermost sea surface water [*Blindheim et al.*, 2000]. Diatoms and coccoliths live in the uppermost part of the water column, in

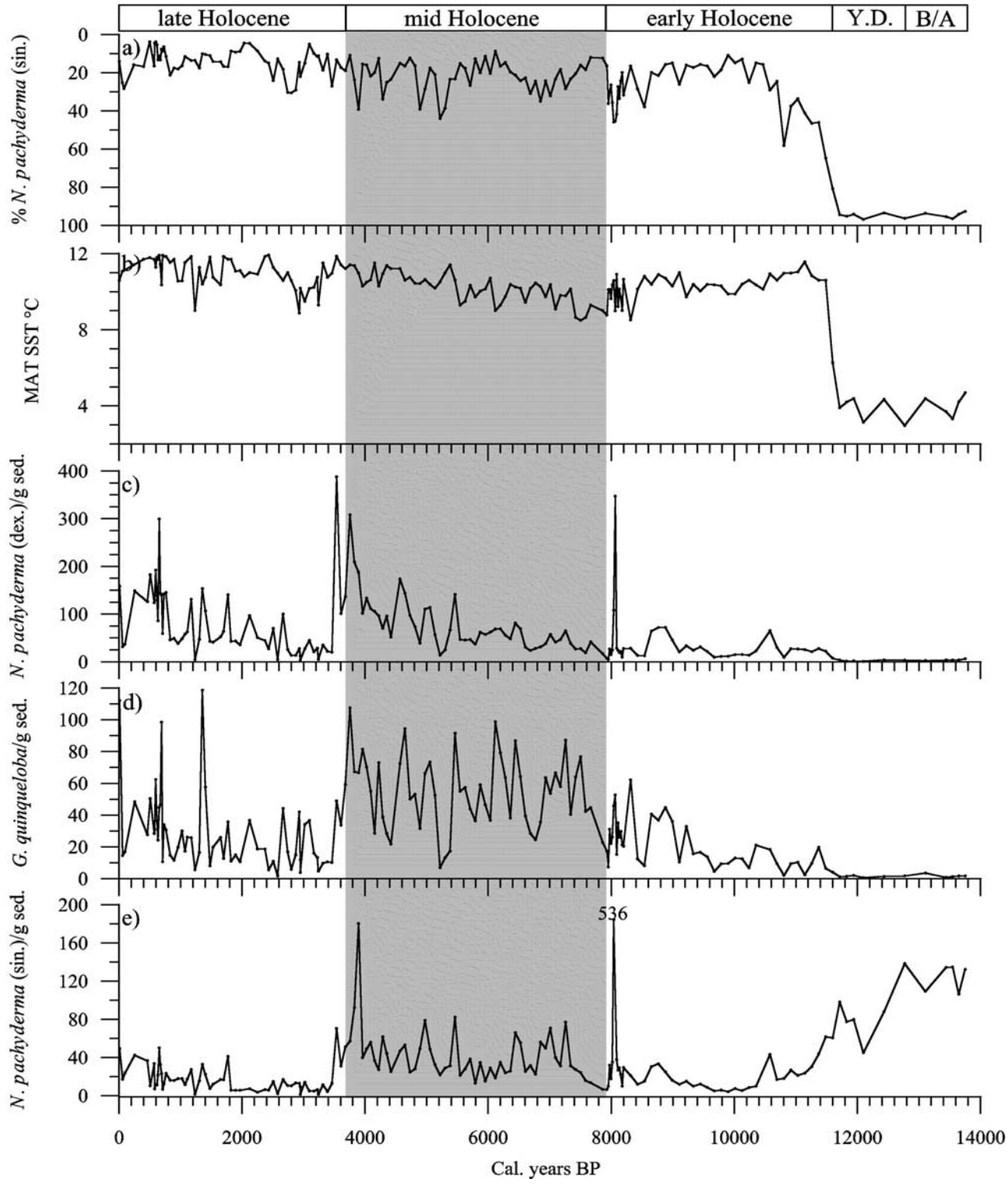

Figure 5. (a) Percentage of *N. pachyderma* (sin.). (b) MAT SST estimate (°C). (c) *N. pachyderma* (dex.)/g sediment. (d) *G. quinqueloba*/g sediment. (e) *N. pachyderma* (sin.)/g sediment. Y.D.: Younger Drays. B/A: Bølling-Allerød.

the photic zone, and will therefore reflect the imprint of warmer Atlantic surface water and the increased summer insolation of the early to mid-Holocene. The somewhat deeper-dwelling foraminifers should instead reflect a signal affected by the increased influence of Arctic water in the subsurface. In such a situation the foraminifera will be a less reliable SST indicator, as their abundance reflects the near-surface water more than the sea surface.

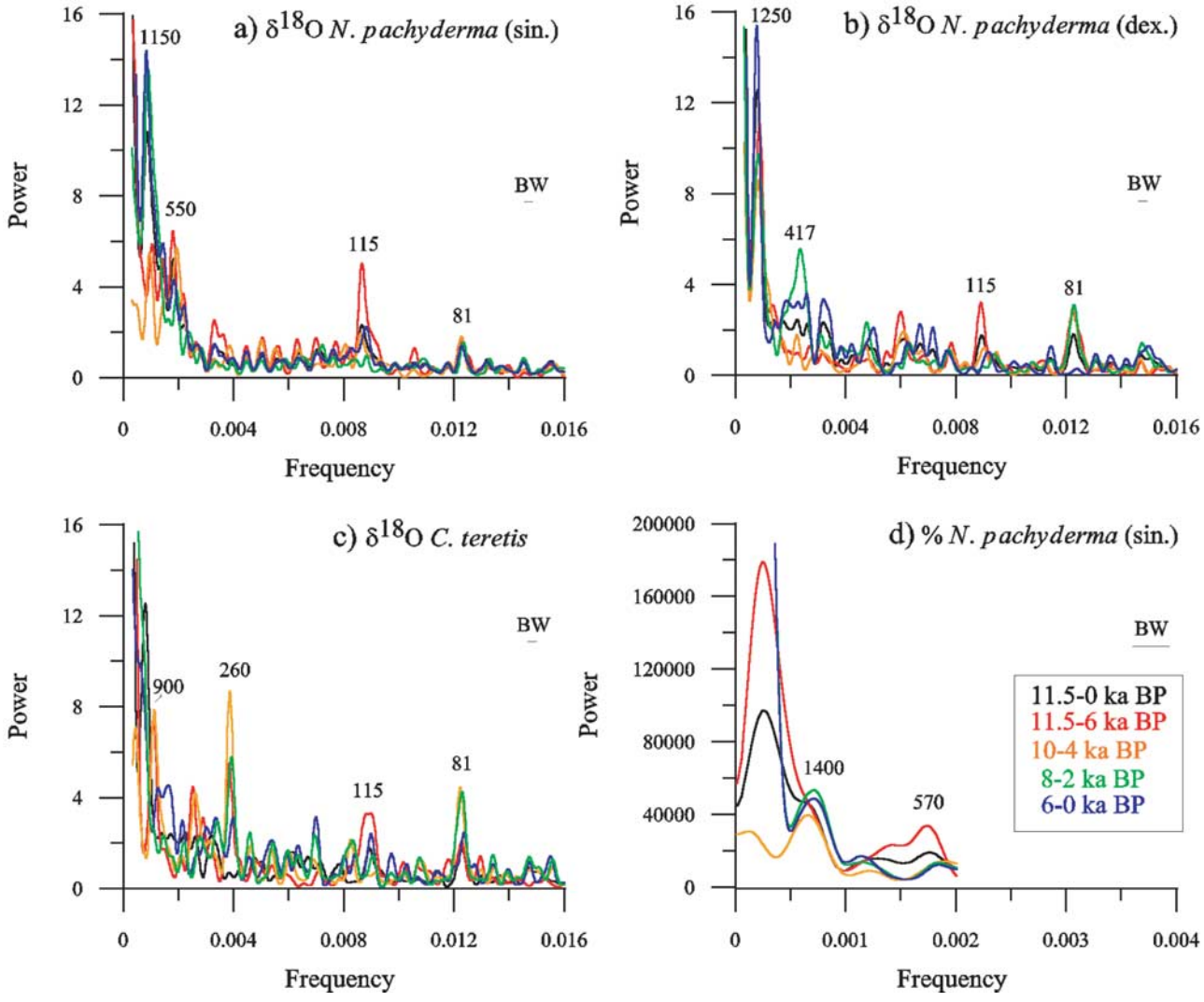

Figure 6. Power spectra (Blackman-Tukey method) of (a) δ^{18}O *N. pachyderma* (sin.), (b) δ^{18}O *N. pachyderma* (dex.), (c) δ^{18}O *C. teretis* and (d) % *N. pachyderma* (sin.). Different studied intervals are represented by different colors: 11.5 ka BP to the present, black; 11.5-6 ka BP, red; 10-4 ka BP, orange; 8-2 ka BP, green; and 6-0 ka BP, blue. BW indicates bandwidth. Note the frequency scale in Figure 6d is different than in Figures 6a–6c.

[20] The late Holocene is characterized by decreased planktic δ^{18}O, increased planktic $\Delta\delta^{18}$O, a lower content of *G. quinqueloba* and planktic foraminifers in general, and higher SST values (Figures 3, 4, and 5; Table 2). These changes suggest an increased influence of Atlantic water masses and reduced importance of Arctic water, possibly due to a general relaxation of the atmospheric forcing (weaker and/or more variable westerlies). A change in the subsurface water from Arctic to Atlantic influence explains the apparent shift to locally warmer conditions at about 4 ka BP, and the opposition of this signal to other marine and terrestrial results. A marked change in climatic conditions at about 4 ka BP is well known from the literature. In north Africa, a decrease in monsoon activity, possibly related to the weakening of summer insolation throughout the Holocene, induced a change from wet to dry conditions at approximately 5-4 ka BP [*Kutzbach et al.*, 1998; *Lamb et al.*, 2000; *deMenocal et al.*, 2000]. The vegetation pattern in northern Fennoscandia changed, the deviation of summer temperatures from modern Scandinavian values decreased, and neoglaciation of Fennoscandia, Svalbard and Franz Josef Land area began [*Dahl and Nesje*, 1996; *Svendsen and Mangerud*, 1997; *Lubinski et al.*, 1999; *Seppä and Hammarlund*, 2000].

[21] Decreasing benthic δ^{18}O generally corresponds with increased planktic δ^{18}O at the study location (Figure 3b). If the observed variability is related to temperature, a change of up to ~3.5°C in deepwater temperature must be explained [*Shackleton*, 1974]. As the lateral distribution of Arctic water expands, the increased contribution of these cold and fresh subsurface waters might act as a lid, thereby reducing the exchange of bottom water and increasing the deepwater temperature. Over the past few decades, a warming of the Norwegian Sea Deep Water (NSDW) has been registered,

apparently connected to the prevailing positive NAO situation [*Dickson et al.*, 1996; *Østerhus and Gammelsrød*, 1999]. However, the effect of the recent NAO pattern on deepwater temperatures is too small to explain the variability observed in the benthic $\delta^{18}O$. If the vertical distribution of Atlantic waters changes so that the boundary zone between relatively warm Atlantic water (~6°C) [*Blindheim*, 1990] and the colder NSDW (~−0.5°C) [*Blindheim*, 1990] is forced to greater depths, large changes in temperature might be possible. However, the presumed increase in bottom water temperature is recorded at the same time as our evidence shows Arctic waters to be of increased influence at the subsurface. This makes it unlikely that the warmer Atlantic waters would have penetrated so deep as to influence bottom temperatures at more than 1 km water depth.

[22] A more plausible explanation for the isotope trends might be that benthic $\delta^{18}O$ values are influenced by waters carrying a signal that changes due to variable influence of brine water from the Arctic Ocean. The intermediate depth brine water, which forms by salt exclusion during sea ice formation, will follow the predominant currents through the Fram Strait and around the Nordic Seas, and should thereby influence bottom waters at the Vøring Plateau. During transport, the isotopic signature would likely be altered as it mixes with the surrounding water at the interfaces, but it should still give rise to rather decreased values. A positive NAO will increase the freshwater flux to the Arctic Ocean and increase the ice flux through Fram Strait [*Kwok and Rothrock*, 1999]. Persisting through time such a situation might give rise to the gradually decreased benthic $\delta^{18}O$ values reflected in parts of the early Holocene and mid-Holocene (Figure 3b), as formation of new sea ice will increase the rate of brine water formation. During the late Holocene, one might assume decreased discharge of the Russian Arctic rivers and reduced sea ice flux through the Fram Strait. Brine water formation would therefore have decreased, as reflected by increased benthic $\delta^{18}O$ (Figure 3b). Driftwood studies from the Arctic region suggest a westward shift of the Transpolar Drift in the last 4 kyr [*Dyke et al.*, 1997], supporting the assumption of reduced ice flux through the Fram Strait. Brine water formation due to deglacial meltwater supply resulted in the most extreme episodes of decreased benthic $\delta^{18}O$, recorded during the Younger Drays (Figure 3b). This event is interpreted as the last imprint of the more extreme variability known from the area during glacial times [*Dokken and Jansen*, 1999].

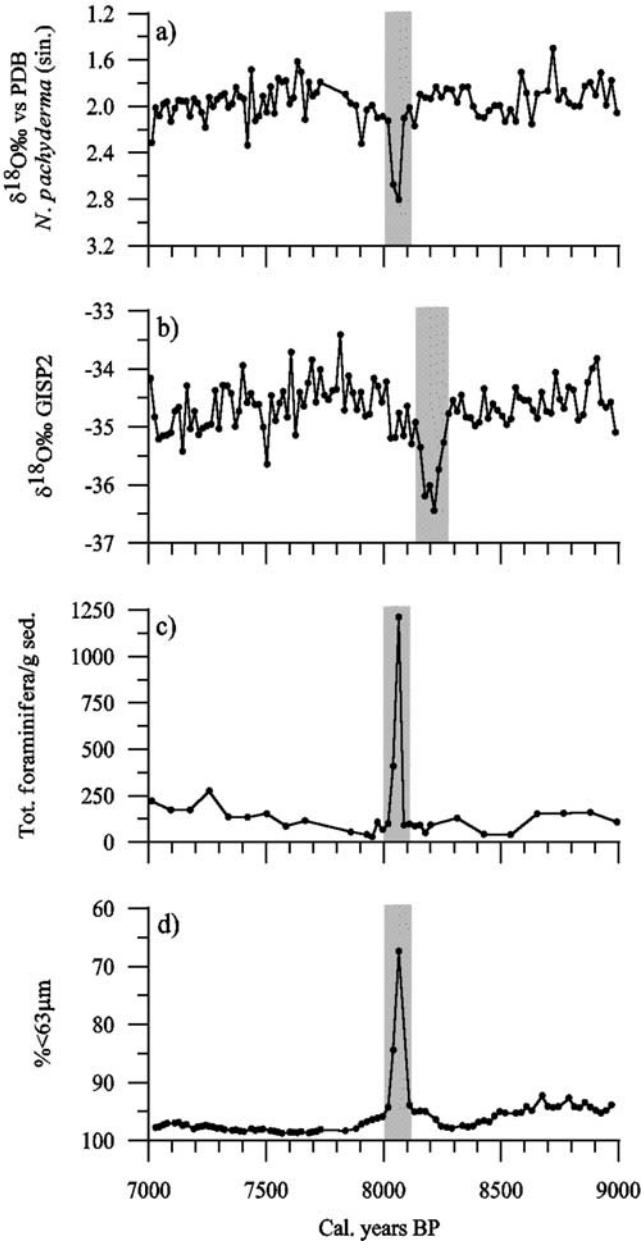

Figure 7. Details of the 8.2 ka BP event. (a) *N. pachyderma* (sin.) $\delta^{18}O$ in ‰ vs. PDB. (b) Oxygen isotope values from GISP2 [*Stuiver et al.*, 1995]. (c) Total amount of foraminifera/g sediment. (d) Percentage of material <63 μm.

4.2. The 8.2 ka BP Event

[23] Around 8100 BP, the planktic $\delta^{18}O$ values of *N. pachyderma* (sin.) culminate in the most extreme cold event of the Holocene (Figure 3b). At the same time, there is a large increase in the amount of foraminifers in the sediment (Figures 5c–5e and 7c). The event is also characterized by an increased percentage of coarser grains, indicating increased winnowing due to stronger bottom current activity or increased ice rafting activity (Figure 7d). The interval of enriched $\delta^{18}O$ in *N. pachyderma* (sin.) is rather abrupt in nature, with the extreme part restricted to a period of about 70 years. During the peak of this cooling, a slight warming recorded in the $\delta^{18}O$ of dextral *N. pachyderma* (sin.) may be the result of different calcification seasons between the two coiling morphotypes. *N. pachyderma* (dex.) generally calcifies during warmer conditions than the left coiling form, and therefore the most extreme values will not be recorded by this taxon if the cooling is not equally distributed through the year. A shorter but more intense summer season may have been recorded by the dextral *N. pachyderma*. Similarities are seen between the $\delta^{18}O$ from *N. pachyderma* (sin.) and the cold event at 8.2 ka BP in the $\delta^{18}O$ record from GISP2 [*Stuiver et al.*, 1995] (Figures 7a and 7b). The same event is also well known from other terrestrial and marine records from the North Atlantic region [*Alley et al.*,

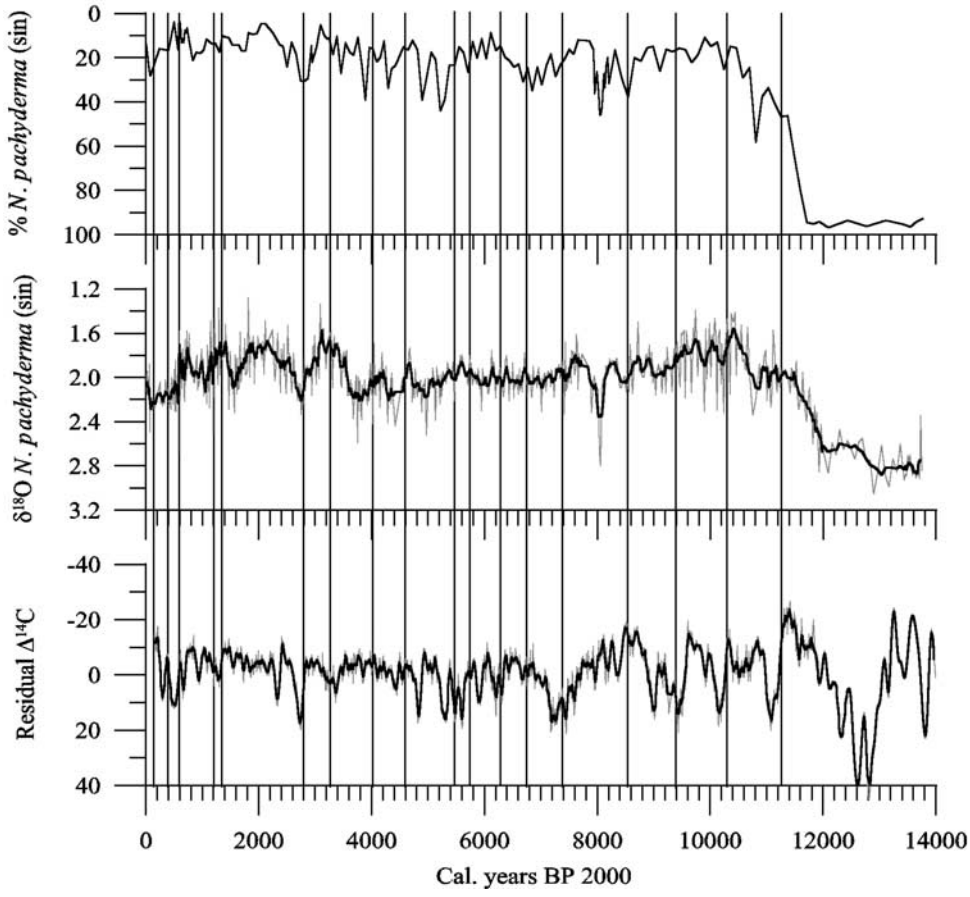

Figure 8. Relative abundance of *N. pachyderma* (sin.) and *N. pachyderma* (sin.) $\delta^{18}O$ from MD95-2011 plotted against residual $\Delta^{14}C$ [*Stuiver et al.*, 1998]. Vertical lines indicate peak ice drift events as recorded by *Bond et al.* [2001].

1997; *Bond et al.*, 1997; *Klitgaard-Kristensen et al.*, 1998; *von Grafenstein et al.*, 1998; *Barber et al.*, 1999; *Nesje and Dahl*, 2001]. In core MD95-2011, the event represents a cooling of about 3°C, a change somewhat larger than the value estimated by *Klitgaard-Kristensen et al.* [1998]. An apparent 150-year discrepancy is seen between the timing of our event and the 8.2 ka BP event in GISP2. This is probably the result of uncertainties in the age model, since few dates are available to precisely constrain this interval. The abrupt cooling event at 8.2 ka BP is thought to be related to a disturbance of the thermohaline circulation, as a response to freshwater perturbation after the final outburst of Lakes Agassiz and Ojibway [*Barber et al.*, 1999].

4.3. Holocene Climate Periodicity

[24] The relative abundance of *N. pachyderma* (sin.) and the *N. pachyderma* (sin.) $\delta^{18}O$ record has been compared to residual $\Delta^{14}C$ [*Stuiver et al.*, 1998], and with ice drift events in the North Atlantic reported by *Bond et al.* [2001] (Figure 8). Both solar activity and the rate of deep water formation influence the $\Delta^{14}C$ [*Stuiver et al.*, 1998; *Bond et al.*, 2001]. *Bond et al.* [2001] argue that Holocene climate variability at millennial and centennial timescales is driven by solar forcing, as the flux of cosmogenic nuclides seems to correlate to the ice drift events. Changes in NADW production are suggested as an additional mechanism for amplifying the solar signals and transmitting them globally. Our records do not show similar results. The correlation between $\Delta^{14}C$ and the MD95-2011 records is poor ($\Delta^{14}C$ vs. $\delta^{18}O$ (*N. pachyderma* (sin.)) correlation coefficient = 0.23). Major changes recorded in the MD95-2011 record are not always represented by ice rafting events in the *Bond et al.* [2001] records, and some of the more pronounced ice rafting events are only represented by small changes in the MD95-2011 records (Figure 8). Thus our comparison between the North Atlantic ice drift events (one of the main sources is expected to be the Nordic Seas) and climate proxies from the Nordic Seas do not support the use of North Atlantic ice drift events as regional climate indicators.

[25] Discussions on the periodic behavior of Holocene climate have concentrated on variability centered on 1500, 1000 and 550 years, periods reportedly found in marine and terrestrial ice core records from the North Atlantic region [e.g., *Stuiver et al.*, 1995; *Bond et al.*, 1997; *Bianchi and McCave*, 1999; *Chapman and Shackleton*, 2000]. *Bond et al.* [1997] have argued that Holocene variability is simply a pervasive, subdued expression of the more pronounced millennial scale variability of the last glacial period, possibly related to changes in the thermohaline circulation, while *Schulz* [2002] has argued against such a possibility. Taking

into account uncertainties in the age model and in the exact period of the expected signals, variability in individual proxy records from MD95-2011 may be connected to these cycles (Figure 6). For example the 1400 year-long period seen in the % *N. pachyderma* (sin.) abundance record is close to the 1500-year cycle, while variability centered on 1250, 1150 and 900 years might be connected to the 1000 year period, or even to the 1500 year cycle. Similarly, 570, 550 and 420 year cycles bear resemblance to the reported 550 years periodicity. However, several aspects of our data contradict such an interpretation. First, the 1400-year period is not recorded as a clear signal, and it is only evident in the lower resolution % *N. pachyderma* record. The 1500 year period is also absent in the Holocene bidecadal $\delta^{18}O$ record from GISP2 [*Stuiver et al.*, 1995]. With increased resolution of North Atlantic ice drift records [*Bond et al.*, 1997], *Bond et al.* [2001] no longer argue for a strong persistent 1500 year Holocene climate periodicity. Second, all our results are from the same core and are based on the same age model. The internal variations reflect real differences in periodicity and can not be explained by uncertainties in the age model, as can discrepancies between results from two different cores. Third, the strength of the periodic behavior is not consistent through time. Shorter periodicities seem to have dominated in the early and mid-Holocene, while longer periods are more pronounced in later intervals (planktic records). For benthic $\delta^{18}O$, the longer 900-year period is recognized only in the older parts. The 260-year period is only seen in the benthic $\delta^{18}O$, and it is best recorded in the older intervals. A period of 115 year is seen in all $\delta^{18}O$ records during the 11.5-6 ka BP interval, and might indicate some sort of consistent behavior during the early part of the Holocene. Climate variability at approximately this frequency is known from several studies [e.g., *Stocker and Mysak*, 1992; *Stuiver et al.*, 1995; *Shabalova and Weber*, 1999], but possible driving forces and their climatic significance are not well known. To conclude, the high-resolution records from MD95-2011 do not provide any evidence for a consistent cyclic behavior of Holocene climate at millennial or centennial timescale.

[26] At multidecadal timescales, all $\delta^{18}O$ records show increased spectral power at a period of about 81-year (Figures 6a–6c). This 81-year signal seems to be rather consistent through time. Except for the 8-2 ka BP interval of the *N. pachyderma* (dex.) $\delta^{18}O$ record, it is well represented in all investigated intervals. Several papers have reported variability at frequencies of around 80 years, including in tree ring records, ice core records, peat stratigraphy, and historical and instrumental records [*Briffa et al.*, 1992; *Schlesinger and Ramankutty*, 1994; *Mahasenan et al.*, 1997; *Chambers and Blackford*, 2001]. Common to these studies is the limited length of the available records, spanning from less than 150 years to about 2 kyr. In contrast, the MD95-2011 $\delta^{18}O$ signal is present throughout the last 11.5 kyr. The length of the period ($\sim$80 years) might indicate a possible connection to the solar Gleissberg cycle [e.g., *Ribes*, 1990; *Waple*, 1999; *Chambers and Blackford*, 2001]. Alternative explanations tend to invoke an internal oscillation of the atmospheric-ocean system or a connection to the thermohaline circulation [*Stocker and Mysak*, 1992; *Delworth et al.*, 1993; *Mann et al.*, 1995; *Schlesinger and Ramankutty*, 1994; *Mahasenan et al.*, 1997]. The 81-year period cannot explain the large-scale variability during the Holocene, but it may be of importance for understanding some of the underlying small-scale variability.

5. Summary and Conclusions

[27] Based on evidence presented here from IMAGES core MD95-2011, the following characterizations and conclusions can be made. During the early and mid-Holocene, generally cold subsurface conditions occurred due to a location of this site closer to the Arctic front as stronger westerlies gave rise to an eastward migration of subsurface Arctic water. The influence of Atlantic water subsequently increased during the late Holocene due to a general relaxation of the atmospheric forcing. As the atmospheric forcing changed, the changing influence of Arctic intermediate brine water brought about unstable bottom water conditions.

[28] The 8.2 ka BP cold event is well represented in the records from the Vøring plateau. This abrupt cooling event is thought to be related to a disturbance of the thermohaline circulation, as a response to freshwater perturbation after the final outburst of Lakes Agassiz and Ojibway.

[29] Changing solar irradiance can not explain the Holocene climate changes seen in our Nordic Seas records. Neither is there any clear connection between climate changes in the Nordic Seas and North Atlantic ice drift events.

[30] Spectral analysis reveals no consistent signal of periodic climate variability of millennial or centennial timescale throughout the Holocene at this location. On multidecadal timescales, weak evidence exists for consistent variability with a period of approximately 81-year throughout the last 11.5 kyr. This 81-year cycle may be connected to the solar Gleissberg cycle, a result of internal oscillations of the atmospheric-ocean system, or related to changes in the thermohaline circulation.

[31] **Acknowledgments.** We thank Dag Inge Blindheim, Odd Hansen and Rune Søraas for laboratory assistance. Trond M. Dokken documented the position of the Vedde ash layer. Martin W. Miles performed MTM and MEM analysis (results not shown) and commented on the manuscript. The study was performed with financial support from The Research Council of Norway and the European Commission as part of the Holocene project. We thank Lloyd Keigwin and Mark Chapman for contributing with constructive reviews.

References

Alley, R. B., P. A. Mayewski, T. Sowers, M. Stuiver, K. C. Taylor, and P. U. Clark, Holocene climate instability: A prominent event 8200 yr. ago, *Geology*, *25*(6), 483–486, 1997.

Appleby, P. G., and F. Oldfield, Application of Lead-210 to sedimentation studies, in *Uranium-Series Disequilibrium*, *Applications to Earth*, *Marine*, *and Environmental Sciences*, edited by I. Ivanovich and R. S. Harmon, pp. 732–778, Clarendon, Oxford, UK, 1992.

Barber, D. C., et al., Forcing of the cold event of 8200 years ago by catastrophic drainage of Laurentide lakes, *Nature*, *400*, 344–348, 1999.

Barlow, L. K., J. C. Rogers, M. C. Serreze, and R. G. Barry, Aspects of climate variability in the North Atlantic sector: Discussion and relation to the Greenland Ice Sheet Project 2 high-resolution isotopic signal, *J. Geophys. Res.*, *102*(C12), 26,333–26,344, 1997.

Bianchi, G. G., and I. N. McCave, Holocene periodicity in North Atlantic climate and deep-ocean flow south of Iceland, *Nature*, *397*, 515–517, 1999.

Birks, C. J. A., A Younger Holocene-Holocene diatom record of sea-surface temperatures and oceanographic changes from core MD95-2011, Vøring Plateau, thesis, Dep. of Geol., Univ. of Bergen, Bergen, Norway, 2001.

Blackman, R. B., and J. W. Tukey, *The measurement of Power Spectra From the Point of View of Communicating Engineering*, Dover, Mineola, N. Y., 1958.

Blindheim, J., Arctic Intermediate Water in the Norwegian Sea, *Deep Sea Res.*, *37*(9), 1475–1489, 1990.

Blindheim, J., V. Borokov, B. Hansen, S. A. Malmberg, W. R. Turrell, and S. Østerhus, Upper layer cooling and freshening in the Norwegian Sea in relation to atmospheric forcing, *Deep Sea Res., Part I*, *47*, 655–680, 2000.

Bond, G., W. Showers, M. Cheseby, R. Lotti, P. Almasi, P. deMenocal, P. Priore, H. Cullen, I. Hajdas, and G. Bonani, A pervasive millennial-scale cycle in North Atlantic Holocene and glacial climates, *Science*, *278*, 1257–1266, 1997.

Bond, G., et al., Persistent solar influence on North Atlantic climate during the Holocene, *Science*, *294*, 2130–2136, 2001.

Briffa, K. R., P. D. Jones, T. S. Bartholin, D. Eckstein, F. H. Schweingruber, W. Karlén, P. Zetterberg, and M. Eronen, Fennoscandian summers from AD 500: Temperature changes on short and long timescales, *Clim. Dyn.*, *7*, 111–119, 1992.

Calvo, E., J. Grimalt, and E. Jansen, High resolution U_{37}^{K} sea surface temperature reconstruction in the Norwegian Sea during the Holocene, *Quat. Sci. Rev.*, *21*, 1385–1394, 2002.

Campbell, I. D., C. Campbell, J. M. Apps, N. N. Rutter, and A. B. G. Bush, Late Holocene ~1500 yr climatic periodicities and their implications, *Geology*, *26*(5), 471–473, 1998.

Chambers, F. M., and J. J. Blackford, Mid- and Late-Holocene climatic changes: A test of periodicity and solar forcing in proxy-climate data from blanket peat bogs, *J. Quat. Sci.*, *16*(4), 329–338, 2001.

Chapman, M. R., and N. Shackleton, Evidence of 550-year and 1000-year cyclicities in North Atlantic circulation patterns during the Holocene, *The Holocene*, *10*(3), 287–291, 2000.

Craig, H., and L. I. Gordon, Deuterium and oxygen-18 variations in the ocean and the marine atmosphere, in *Stable Isotopes in the Oceanographic Studies and Paleotemperatures*, edited by E. Tongiorgi, pp. 9–130, Cons. Naz. Delle Ric., Lab. Di Geol. Nucl., Pisa, 1965.

Dahl, S. O., and A. Nesje, A new approach to calculating Holocene winter precipitation by combining glacier equilibrium-line altitudes and pine-tree limits: A case study from Hardangerjøkulen, central southern Norway, *The Holocene*, *6*(4), 381–398, 1996.

Delworth, T., S. Manabe, and R. J. Stouffer, Interdecadal variation of the thermohaline circulation in a coupled ocean-atmosphere model, *J. Clim.*, *6*, 1993–2011, 1993.

deMenocal, P., J. Ortiz, T. Guilderson, and M. Sarnthein, Coherent high- and low-latitude climate variability during the Holocene warm period, *Science*, *288*, 2198–2202, 2000.

Dickson, R., J. Lazier, J. Meinicke, P. Rhines, and J. Swift, Long-term coordinated changes in the convective activity of the North Atlantic, *Prog. Oceanogr.*, *38*, 241–295, 1996.

Dokken, T. M., and E. Jansen, Rapid changes in the mechanism of ocean convection during the last glacial period, *Nature*, *401*, 458–461, 1999.

Dyke, A. S., J. England, E. Reimnitz, and H. Jetté, Changes in driftwood delivery to the Canadian Arctic archipelago: The hypothesis of postglacial oscillation of the transpolar drift, *Arctic*, *50*(1), 1–16, 1997.

Fairbanks, R. G., A 17, 000-year glacio-eustatic sea level record: Influence of glacial melting rates on the Younger Drays event and deep-ocean circulation, *Nature*, *342*, 637–642, 1989.

Grönvold, K., N. Óskarsson, S. J. Johnsen, H. B. Clausen, C. U. Hammer, G. Bond, and E. Bard, ash layers from Iceland in the Greenland GRIP ice core correlated with oceanic and land sediments, *Earth Planet. Sci. Lett.*, *135*, 149–155, 1995.

Grootes, P. M., and M. Stuiver, Oxygen 18/16 variability in Greenland snow and ice with 10^{-3}- to 10^{5}-year time resolution, *J. Geophys. Res.*, *102*(C12), 26,455–26,470, 1997.

Grootes, P. M., M. Stuiver, J. W. C. With, S. Johnsen, and J. Jouzel, Comparison of oxygen isotope records from the GISP2 and GRIP Greenland ice cores, *Nature*, *366*, 552–554, 1993.

Harrison, S. P., I. C. Prentice, and P. J. Bartlein, 1992, Influence of insolation on atmospheric circulation in the North-Atlantic sector—Implications of general-circulation model experiments for the late Quaternary climatology of Europe, *Quat. Sci. Rev.*, *11*, 283–299, 1992.

Haykin, S., *Nonlinear Methods of Spectral Analysis*, 2nd ed., Springer-Verlag, New York, 1983.

Hurrell, J. W., Decadal trends in the North Atlantic oscillation: Regional temperatures and precipitation, *Science*, *269*, 676–679, 1995.

Johannessen, T., Stable isotopes as climate indicators in ocean and lake sediments, PhD thesis, Dep. of Geol., Univ. of Bergen, Bergen, Norway, 1992.

Johannessen, T., E. Jansen, A. Flatøy, and A. C. Ravelo, The relationship between surface water masses, oceanographic fronts and paleoclimatic proxies in surface sediments of the Greenland, Iceland and Norwegian Seas, in *Carbon Cycling in Glacial Ocean: Constraints on the Ocean's Role in Global Change*, vol. 1 17, *NATO ASI Ser.*, edited by R. Zahn, M. Kominski, and L. Labyrie, pp. 61–85, Springer-Verlag, New York, 1994.

Karlén, W., Scandinavian glacial and climatic fluctuations during the Holocene, *Quat. Sci. Rev.*, *7*, 199–209, 1988.

Keigwin, L. D., and R. S. Pickart, Slope water current over the Laurentian Fan on interannual to millennial time scales, *Science*, *286*, 520–523, 1999.

Klitgaard-Kristensen, D., H. P. Sejrup, H. Haflidason, S. Johnsen, and M. Spurk, A regional 8200 cal. yr BP cooling event in northwest Europe, induced by final stages of the Laurentide ice-sheet deglaciation?, *J. Quat. Sci.*, *13*(2), 165–169, 1998.

Koç, N., E. Jansen, and H. Haflidason, Paleoceanographic reconstructions of surface ocean conditions in the Greenland, Iceland and Norwegian Seas through the last 14 ka based on diatoms, *Quat. Sci. Rev.*, *12*, 115–140, 1993.

Koç Karpuz, N., and E. Jansen, A high-resolution diatom record of the last deglaciation from the SE Norwegian Sea: Documentation of rapid climatic changes, *Paleoceanography*, *7*(4), 499–520, 1992.

Kutzbach, J., R. Gallimore, S. Harrison, P. Behling, R. Selin, and F. Laarif, Climate and biome simulations for the past 21,000 years, *Quat. Sci. Rev.*, *17*, 473–506, 1998.

Kwok, R., and D. A. Rothrock, Variability of Fram Strait ice flux and North Atlantic oscillation, *J. Geophys. Res.*, *104*(C3), 5177–5189, 1999.

Lamb, A. L., M. J. Leng, H. F. Lamb, and M. U. Mohammed, A 9000-year oxygen and carbon isotope record of hydrological change in a small Ethiopian crater lake, *The Holocene*, *10*(2), 167–177, 2000.

Levitus, S., *World Ocean Atlas (WOA94)*, Ocean Clim. Lab., Natl. Oceanogr. Data Cent., Boulder, Colo., 1994.

Lubinski, D. J., S. L. Forman, and G. H. Miller, Holocene glacier and climate fluctuations on Franz Josef Land, Arctic Russia, 80°N, *Quat. Sci. Rev.*, *18*, 85–108, 1999.

Mahasenan, N., R. G. Watts, and H. Dowlatabadi, Low-frequency oscillations in temperature-proxy records and implications for recent climate change, *Geophys. Res. Lett.*, *24*(5), 563–566, 1997.

Mann, M. E., J. Park, and R. S. Bradley, Global interdecadal and century-scale climate oscillations during the past five centuries, *Nature*, *378*, 266–270, 1995.

Mayewski, P. A., L. D. Meeker, M. S. Twickler, S. Withlow, Q. Yang, W. B. Lyons, and M. Prentice, Major features and forcing of high-latitude Northern Hemisphere atmospheric circulation using a 11,0000-year-long glaciochemical series, *J. Geophys. Res.*, *102*(C12), 26,345–26,366, 1997.

Mork, K. A., and J. Blindheim, Variations in the Atlantic inflow to the Nordic Seas, 1955–1996, *Deep Sea Res., Part I*, *47*, 1035–1057, 2000.

Nesje, A., and S. O. Dahl, Late glacial and Holocene glacier fluctuations and climate variations in western Norway—A review, *Quat. Sci. Rev.*, *12*, 255–261, 1993.

Nesje, A., and S. O. Dahl, The Greenland 8200 cal. yr BP event detected in loss-on-ignition profiles in Norwegian lacustrine sediment sequences, *J. Quat. Sci.*, *16*(2), 155–166, 2001.

Nesje, A., Ø. Lie, and S. O. Dahl, Is the North Atlantic Oscillation reflected in Scandinavian glacier mass balance records?, *J. Quat. Sci.*, *15*(6), 587–601, 2000.

Østbø, M., Oxygen isotope characteristics of water masses and mixing in the Nordic Seas, thesis, Fac. of Phys., Inf. and Math., Nor. Univ. of Sci. and Technol., 2000.

Østerhus, S., and T. Gammelsrød, The abyss of the Nordic Seas is warming, *J. Clim.*, *12*, 3297–3304, 1999.

Paillard, D., L. Labeyrie, and P. Yiou, Macintosh program performs time-series analysis, *Eos Trans. AGU*, *TI.* 379, 1996.

Ribes, E., Astronomical determinations of the solar variability, *Philos. Trans. R. Soc. London, Ser. A*, *330*, 487–497, 1990.

Schlesinger, M. E., and N. Ramankutty, An oscillation in the global climate system of period 65–70 years, *Nature*, *367*, 723–726, 1994.

Shabalova, M. V., and S. L. Weber, Patterns of temperature variability on multidecadal to centennial timescales, *J. Geophys. Res.*, *104*(D24), 31,023–31,041, 1999.

Shackleton, N. J., Attainment of isotopic equilibrium between ocean water and the benthonic foraminifera genus *Uvigerina*: Isotopic changes in the ocean during the last glacial, *Colloq. Int. C. N. R. S.*, *219*, 203–209, 1974.

Schulz, M., On the 1470-year pacing of Dansgaard-Oeschger warm events, *Paleoceanography*, *17*(2), 1014, doi:10.1029/2000PA000571, 2002.

Schulz, M., and A. Paul, Holocene climate variability on centennial-to-millennial time scales: 1. Climate records from the North-Atlantic realm, in *Climate Development and History of the North Atlantic Realm*, edited by G. Wefer et. al., pp. 41–54, Springer-Verlag, New York, 2002.

Seppä, H., and D. Hammarlund, Pollen-stratigraphical evidence of Holocene hydrological change in northern Fennoscandia supported by independent isotopic data, *J. Paleolimnol.*, *24*, 69–79, 2000.

Stocker, T. F., and L. A. Mysak, Climatic fluctuations on the century time scale: A review of high-resolution proxy data and possible mechanisms, *Clim. Change*, *20*, 227–250, 1992.

Stuiver, M., and T. F. Braziunas, Modeling atmospheric ^{14}C influences and ^{14}C ages of marine samples to 10,000 BC, *Radiocarbon*, *35*(1), 137–189, 1993.

Stuiver, M., P. M. Grootes, and T. F. Braziunas, The GISP2 $\delta^{18}O$ climate record of the past 16,500 years and the role of the Sun, ocean, and volcanoes, *Quat. Res.*, *44*, 341–354, 1995.

Stuiver, M., P. J. Reimer, E. Bard, J. W. Beck, G. S. Burr, K. A. Hughen, B. Kramer, F. G. McCormac, J. V. D. Plicht, and M. Spurk, Intcal98 radiocarbon age calibration 24,000-0 cal BP, *Radiocarbon*, *40*, 1041–1083, 1998.

Svendsen, J. I., and J. Mangerud, Holocene glacial and climatic variations on Spitsbergen, Svalbard, *The Holocene*, *7*(1), 45–57, 1997.

Thompson, D. J., Spectrum estimation and harmonic analysis, *Proc. IEEE*, *70*, 1055–1096, 1982.

von Grafenstein, U., H. Erlenkauser, J. Müller, J. Jouzel, and S. Johnsen, The cold event 8200 years ago documented in oxygen isotope records of precipitation in Europe and Greenland, *Clim. Dyn.*, *14*, 73–81, 1998.

Waple, A. M., The sun-climate relationship in recent centuries: A review, *Prog. Phys. Geogr.*, *23(3), 309–328, 1999.*

C. Andersson and E. Jansen, Bjerknes Centre for Climate Research, Allégaten 55, N-5007 Bergen, Norway. (carin.andersson@geo.uib.no; eystein.jansen@geo.uib.no)

K. Hevrøy, Norsk Hydro ASA, Bergen, Norway. (kjersti.hevroy@hydro.com)

E. Mjelde and B. Risebrobakken, Department of Earth Science, University of Bergen, Allégaten 41, N-5007 Bergen, Norway. (eirik.mjelde@geo.uib.no; bjorg.risebrobakken@geo.uib.no)